

## Parameterisation of ultrasonic echographic images for intraocular tumour differentiation

D. Jegelevičius<sup>1</sup>, A. Lukoševičius<sup>1</sup>, A. Paunksnis<sup>2</sup>, D. Šebeliauskienė<sup>2</sup>

<sup>1</sup>Biomedical Engineering Institute of Kaunas University of Technology  
Studentu str. 50, Kaunas, LT-3031

<sup>2</sup>Department of ophthalmology of Institute for Biomedical Research of Kaunas University of Medicine  
Eivenių str. 2, Kaunas, LT-3007

### Introduction

Differential diagnosis of eye tumours is one of important problems in ophthalmology. Malignant eye tumours have a 0.2 per cent deal in all malignant tumours diagnosed. This percentage is not very high, but in absolute values number of patients per year is considerable. Eye tumours, especially melanomas are dangerous because of metastases. Therefore early differential diagnostic is crucial for treatment and prognosis.

Among instruments of differential diagnosis ultrasound investigation is widely used. Non invasiveness, high resolution, and informativity are the favourite features of ultrasound echography.

There are several indicators used for differentiation of intraocular tumours: geometry, size, shape, and microstructure are frequently used in clinical practice [1, 2]. In addition blood flow, biochemical indicators and other collateral information is also used for clinical decision making [3]. Ultrasound investigation can give very important geometrical and structural parameters of tumour [1, 2].

Lot of research is made on ultrasonic tissue characterisation [1, 2, 4]. Both A scans (one dimensional detected or radiofrequency signals) and B scans (two dimension images) are used for characterisation. Although radiofrequency ultrasonic signal is more enriched by information to compare with detected signal or B-image, in clinical practice radiofrequency signal from commercial scanners is not available. Access to this signal is related with radical interventions into hardware, which is difficult to implement because of integrity of the equipment, safety and other reasons. Of course, the ultrasound RF signals processing is the better way to improve resolution of ultrasound imaging systems [7, 8] and to characterise the tissues.

Therefore advanced methods of secondary processing of echographic B-type images should be developed in order to get all possible information about tumour properties from echographic image. The most promising way of image processing is to use information about the mechanism of image pixel genesis. In other words the processing of image should be provided with regard of ultrasonic echography parameters, such as space-dependent longitudinal and transversal resolution, attenuation, algorithm of formation of pixels from radiofrequency signals and other. Filtration of image and deep texture analysis including space-dependant pixel statistics are issues to be developed further.

The aim of present paper is to develop a set of ultrasonic echographic image parameters to be used in ultrasonic tumour tissue characterisation.

### Origin of echographic image

Ultrasound scanner operates in brightness mode (B-mode) and the brightness represents a map of amplitudes of reflected and scattered ultrasonic signals from tissue as a function of position in the plane being scanned.

The echographic image  $g(x,y)$  can be represented by the use of the two-dimensional function of the object acoustical properties  $f(x,y)$ :

$$g(x, y) = \iint h(x, y) \cdot f(x, y) dx dy + n(x, y), \quad (1)$$

where  $n$  is a noise function and  $h$  is the impulse response function.

Since  $h$  also represents the spread of a point object in the image, or system response to the point scatterer it is called the Point Spread Function (PSF) of the imaging system [5]. Equation (1) shows that distribution of acoustical properties (mainly acoustic impedance inhomogeneties) is distorted or "blurred" by PSF. It causes the reduction of image resolution and at the same time reduces possibilities for tumour tissue characterisation by evaluation of its fine microstructure. Therefore one should look for possibilities to restore image by the use a-priori information about PSF. One of the most evident methods is inverse filtration in frequency domain.

In the Fourier space the equation (1) becomes:

$$G(u, v) = H(u, v) \cdot F(u, v) + N(u, v). \quad (2)$$

This implies that if  $H(u,v)$  is known, we can restore  $f(x,y)$ . The restoration function is usually called inverse filter:

$$H^{-1} = \frac{G(u, v) - N(u, v)}{H(u, v)}. \quad (3)$$

Implementation of inverse filter (3) as well as implementation of other model based correction methods requires the knowledge of PSF and noise. The character of the PSF is determined by the centre frequency and bandwidth of the acoustic signal, aperture, element geometries, detection parameters of radiofrequency pulse and beam forming technique of the transducer. The PSF depends on the attenuation of the tissue and varies depending on the distance by two reasons: divergence of interrogating beam and frequency dependent attenuation. Therefore the ultrasound B-scan image does not describe accurately acoustical properties of the tissue due to the space dependent and "not ideal" PSF.

From the other hand knowledge of PSF allows image restoration techniques [6, 7, 8] to be applied in order to decrease ultrasound image distortion and to increase resolution.

Let's consider in more details PSF origin itself.

### Calculation of point spread function

The Mentor Advent A/B ultrasound system [9] is a typical ophthalmological scanner routinely used for patient eye examinations in Kaunas Eye Clinics. We will estimate PSF of this system by two methods: digital simulation with the use of a-priori information about ultrasonic transducer and "blind" image deconvolution algorithm with the use of the B-scan image properties only.

Table 1. Mentor Advent A/B ultrasound systems B-scan specifications

Probe frequency	11MHz broadband
System frequencies	7.5MHz, 12.5MHz, 15MHz
Gain range	50-90dB
Scan angle	50°
Scan depths	2cm, 3.5cm, 5cm, 7cm
Probe type	Permanently sealed, mechanical sector scanning
Gray scale	256 level
Transducer focus	25 mm
Beam dimensions at axial distance $z_p=1.4$ cm	0.082x0.086cm
Output beam dimensions	0.55cm diameter

Examiner usually is using such ocular ultrasonography system settings: frequency 12.5 MHz, velocity of ultrasonic waves – 1550 cm/s, scan range – 50 mm. The example of B-scan obtained with the use of such settings is presented on Fig.1. The B-scan image is transferred from video output of ultrasound system to personal computer (PC) by the use of frame grabber. Such ultrasound image capture method is quite simple and can be implemented with the most ultrasonic systems. Captured image is of size 640x480 pixels. From this grabbed image calculated pixel size in mm is about 0.16x0.16 for 50 mm scanning range. These calculations were performed using the reference distance scale line on the image (see Fig.1, below A-scan curve).

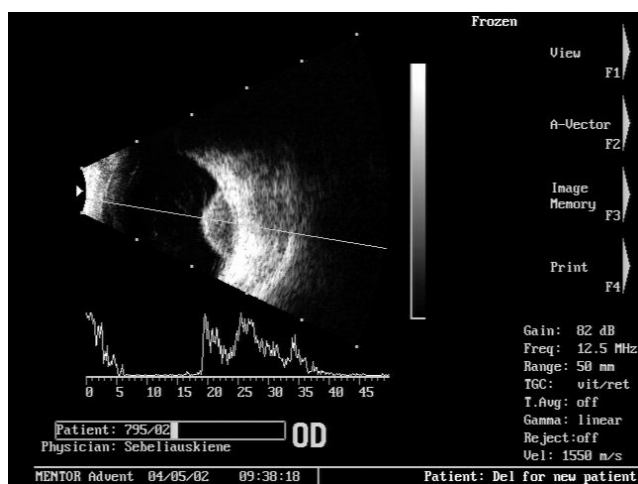


Fig. 1. B-scan image of Mentor Advent A/B ultrasound system

Scanning system interrogates the region of interest of tissue with wide bandwidth ultrasound pulses. The incident

acoustic pulse excites certain volume of tissue. In the plane of scanning it can be represented by three dimensional function which has unequal lateral and axial dimensions (Fig. 2). We had modelled two-way ultrasound pulse propagation and estimated PSF from it. PSF for inverse filtering was analyzed at the distance of 22 mm, which corresponds usually to the middle of the intraocular tumour and therefore is most interesting for the examining physician. Calculations were performed using the method, described by J.A.Jensen [10] with the Field II Matlab toolbox.

A-priori transducer parameters were collected from Mentor Advent system specifications officially available (table 1, [11]). Following parameters were used for modelling:

- Transducer centre frequency 12.5MHz
- Sampling frequency 125MHz
- Size of aperture sampling element 0.025mm
- Geometric focus point 25mm
- Radius of transducer 2.7mm
- Ultrasound velocity 1550m/s

Transducer diameter is not given in specifications, but it was estimated by an iterative way: by fitting beam dimensions presented in specification (table 1).

Ultrasound pulse radio frequency signal form point scatterer in transmit-receive mode calculated at the 22mm distance from transducer is presented on Fig. 2.

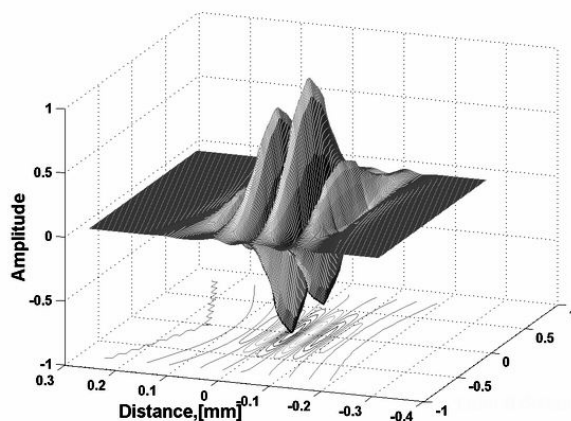


Fig. 2. Ultrasound pulse from point scatterer at the 22 mm from transducer

Since B-scanner uses detected envelope of the radiofrequency signal for visualization, pulse in Fig.2 was detected by the use of Hilbert transform. Resulting envelope, or PSF was calculated by application of Hilbert transform and presented as a contour plot on Fig.3.

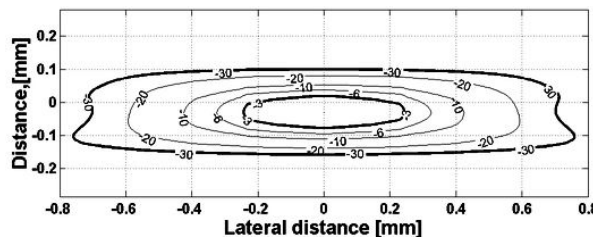


Fig. 3 Point spread function at the 22 mm from the transducer

The PSF calculated from ultrasound field simulations has dimensions about  $0.1 \times 0.5$  mm (at -3dB level) from the Fig.3. Therefore from it we can estimate axial and lateral resolutions for the image. Potential axial resolution is about 0.12mm for the 12.5 MHz frequency (one wavelength) and assuming that ultrasound propagation velocity is 1550m/s.

The PSF got from calculations of ultrasound field (Fig.5, a) was digitized considering image pixel size. The resulting PSF image was got to be of size  $9 \times 9$  pixels 2D image filter. From pixel analysis one can state that image resolution is quite well adjusted to the ultrasound system resolution.

Ultrasound pulse is changing its shape while propagating in tissue. The main reason for it lies in ultrasound transducer properties and beam forming features (transducer diameter, pulse focusing). The attenuation and velocity dispersion are also important for the ultrasound field evaluation in tissue. The attenuation in real scanner is compensated implementing time gain control of the amplifier. Therefore in ultrasound image this compensation exists and in point spread function calculations we do not need to use additional attenuation effect (regarding amplitude of PSF) as PSF is an image feature.

Tissue nonlinearities and frequency dependent attenuation also has influence on PSF, but since there are very limited a-priori information about it and main contribution to the PSF is from transducer side, in present calculations only transducer parameters were taken into account.

Ultrasound field point spread function distribution in space is illustrated in Fig.4. This change causes space variant resolution of the image. Best resolution in lateral and axial directions is at the focus. Focus is at the 25 mm distance what is almost on the bottom of the eye (it is depending on eye ball size), - mostly interesting place for eye physicians. We are using distance 22 mm for calculations, as mentioned before. It is the most common distance form transducer till the middle of the tumour.

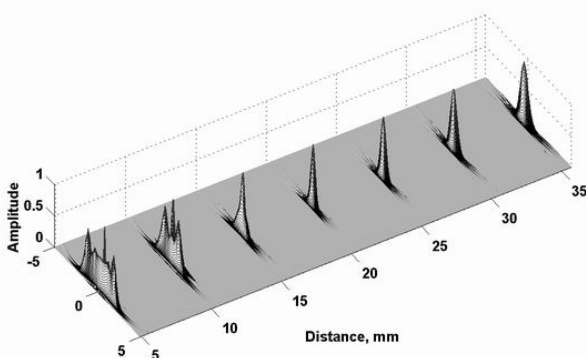


Fig. 4. Modelled ultrasonic transducer's PSF variance in space along scanning line

Another method for point spread function estimation is to use blind image deconvolution algorithm [11]. The algorithm finds an estimate of the true image using partial or no information about the PSF and noise in true image. The algorithm maximizes the likelihood that the resulting image, when convolved with the resulting PSF, is an instance of the blurred image, assuming Poisson noise

statistics. It is done by iterative process. The outputs for this algorithm is restored image and found PSF. PSF size was taken to be  $9$  by  $9$  pixels as the size of the modelled PSF. The initial PSF was taken to be all 1. On the Fig.5, b) one can see estimated PSF by this algorithm. The calculated PSF from ultrasound pulse modelling is shown for comparison on the Fig.5, a).

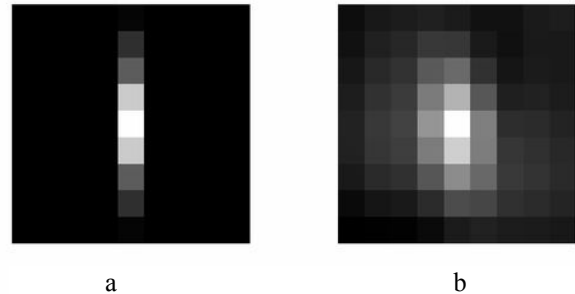


Fig. 5. Calculated PSF ( $9 \times 9$  pixels). a) - result from transducer field calculation; b) - result of blind deconvolution

You can see similarity of these results. Blind deconvolution PSF and modelling PSF shows better resolution in axial direction than in lateral as it was expected and as it is common for ultrasound scanning images.

### Inverse filtering of the image

As described in second section of the article, inverse filtering of the image could be principally the tool for ultrasound image resolution enhancement. Here we will evaluate this technique for Mentor Advent system images.

The inverse image filtering equation given in formulas (2) and (3) could be hardly directly applied to image filtering because in noisy image the term  $N(u,v)/H(u,v)$  may have large magnitude and be instable, so will not be a meaningful restoration of  $f(x,y)$ . Therefore additional conditions should be taken and applied approximate inversion techniques less sensitive to the noise. One way is the use of Wiener filtering (least squares) [5, 6]. It is the optimal trade-off between the inverse filtering and noise smoothing.

The noise and signal ratio must be known prior Wiener filtering using PSF. Evaluation shows it was 0.2. The results of Wiener filtering (or in other words deconvolution) are shown on figure 6. The fragment of original ultrasound image and deconvolved image using modelled PSF (from figure 5, a) are shown. There is seen increase in lateral resolution. This increase quantitatively is illustrated on Fig.7, where calculated autocovariance function [7] of the images in the lateral direction before and after deconvolution is presented. In order to achieve best results the evaluation of the noise to signal ratio should be studied in more details.

The deconvolution using PSF obtained with blind deconvolution algorithm (Fig. 5, b) did not produced better result than using modelled PSF.

### Tumour image texture parameters

Quantitative tumour texture parameters are of decisive importance for the use for classification of tumours type by it's microstructure.



Fig. 6. Original a) and deconvolved b) with modelled PSF fragment of the image

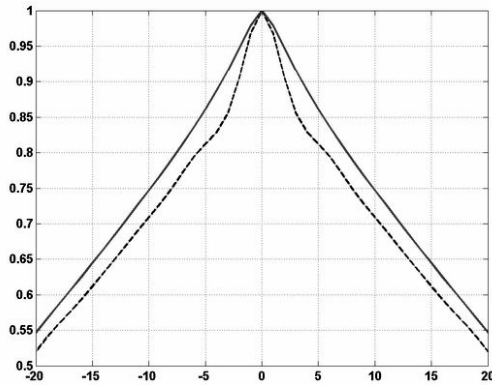


Fig. 7. Increase in lateral resolution,- autocovariance functions in lateral direction (solid line,- before deconvolution, dotted line,- after deconvolution)

The suspected tumour in the ultrasound image is initially identified by the shape and ultrasound reflection intensity [1, 2]. The tumour shape can be described by the geometrical parameters of the eye ultrasound image tumour object, and the ultrasound intensity features can be described by the statistical image object intensity parameters and texture features. Therefore we have two classes of image parameters: geometrical and grey level statistics. Below we'll concern grey level distribution, or so called texture of image. The aim is to derive possible parameters describing tissue image texture and indirectly – tumour microstructure.

We have chosen statistical methods for tumour texture analysis [12, 13]. Statistical methods use second order statistics to model relationships between pixels within the region of interest. The co-occurrence matrices are the most explicit tools for texture statistics analysis and will be used below [12, 13].

Co-occurrence matrix is a spatial grey level dependency matrix. It is the joint probability occurrence of grey levels  $i$  and  $j$  for two pixels with defined spatial relationship in an image. The co-occurrence matrix for displacement vector  $d(dx, dy)$  is a  $G \times G$  ( $G$  is a grey level number in the image) matrix  $P_d$ . The entry  $(i, j)$  of  $P_d$  is the number of occurrences of the pair of grey levels  $i$  and  $j$  which are a distance  $d(dx, dy)$  apart:

$$P_d(i, j) = |\{(r, s), (t, v) : I(r, s) = i, I(t, v) = j\}|, \quad (4)$$

where  $I$  is an image of size  $M \times N$ ,  $(r, s), (t, v) \in N \times M$ ,  $(t, v) = (r + dx, s + dy)$ , and  $||$  is the cardinality of a set.

As an example the co-occurrence matrix was calculated not for all ultrasound image, but only for the outlined tumour image region (see Fig.8 with typical

images of two different tumour types). Co-occurrence matrices calculated for those tumours in Fig. 8 are presented on Fig. 9. Vector defining direction is  $d=0,1$ .

A number of texture parameters can be calculated from the co-occurrence matrices:

- Energy:

$$\sum_i \sum_j P_d^2(i, j); \quad (5)$$

- Entropy:

$$\sum_i \sum_j P_d(i, j) \cdot \log P_d(i, j); \quad (6)$$

- Contrast:

$$\sum_i \sum_j (i - j)^2 \cdot P_d(i, j); \quad (7)$$

- Homogeneity:

$$\sum_i \sum_j \frac{P_d(i, j)}{1 + |i - j|}; \quad (8)$$

- Correlation:

$$\frac{\sum_i \sum_j (i - M_x)(j - M_y) \cdot P_d(i, j)}{S_x \cdot S_y}, \quad (9)$$

where  $M_x, M_y$  are the means and  $S_x, S_y$  are the standard deviations of  $P_d(x)$  and  $P_d(y)$  respectively:

$$P_d(x) = \sum_j P_d(x, j); \quad P_d(y) = \sum_i P_d(i, y). \quad (10)$$

Co-occurrence matrix should be calculated for the given displacement vectors  $d(dx, dy)$ . Varying displacement vector, what mean changing direction and distance, we can estimate statistical anisotropy of the tumour image. The latter possibility is very important and can not be achieved for more sophisticated A-scan processing methods. One can expect certain anisotropy of tumour structure, since it starts to grow on retina towards the middle of the eyeball that is tumour has the prevailing direction of growth, therefore possible anisotropy of cells and microstructure.

For the partial analysis or to reduce computations time it could be chosen direction at 0 degrees. This choice we argue regarding to the ultrasound image and eye peculiarity:

- Ultrasound image resolution is better in axial direction than in lateral, therefore the structure of the tumour is expressed more in this direction too
- Tumour is placed on the bottom of the eye, that is almost perpendicular to the ultrasound beam.

The outlined tumour object on the image should be properly oriented regarding to the co-occurrence matrix calculation direction. Therefore we rotated this object by the degree of the angle between transducer central point (as reference for it is shown by the small triangle in the image left side, see figure 1) and tumour mass centre. In this way we orient tumour image to the texture analysis orientation. It should be pointed out that vectors  $d(dx,dy)$  allows to orient direction of calculation without rotation of image. In principle this is more preferable method, since rotation can introduce some minor re-discretization error.

Two kinds of tumours, manually outlined and cropped from the ultrasound B-scan images, are presented on figure 8 and used for more detail analysis. Tumours are of two different types presenting different cell structures: Fig. 8. a) – spindle cell uveal melanoma, Fig.8. b) – mixed cell uveal melanoma. Some results of texture analysis are presented on Fig.10. The texture parameters were calculated using co-occurrence matrices normalized by the tumour area and varying distance vector  $d(dx,dy)$ , where  $dx=dy$  from 1 to 30 image pixels. The correlations and contrasts coefficients are calculated for four directions: 0, 45, 90 and 135 degrees. The periodicity of curves and extremums represents structure of the tumour image texture. We can see that in some directions periodicity is repeatable and in other it changes.

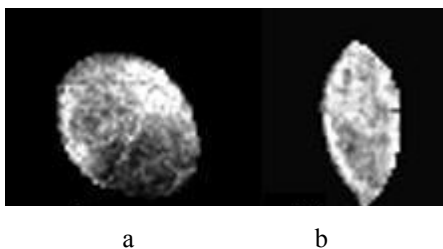


Fig. 8. Outlined tumours from ultrasound B-scan images: a) – spindle cell uveal melanoma, b) – mixed cell uveal melanoma

It should be done more quantitative calculations of tumour images for qualitative evaluation of these differences and parameters significance to the tumours type.

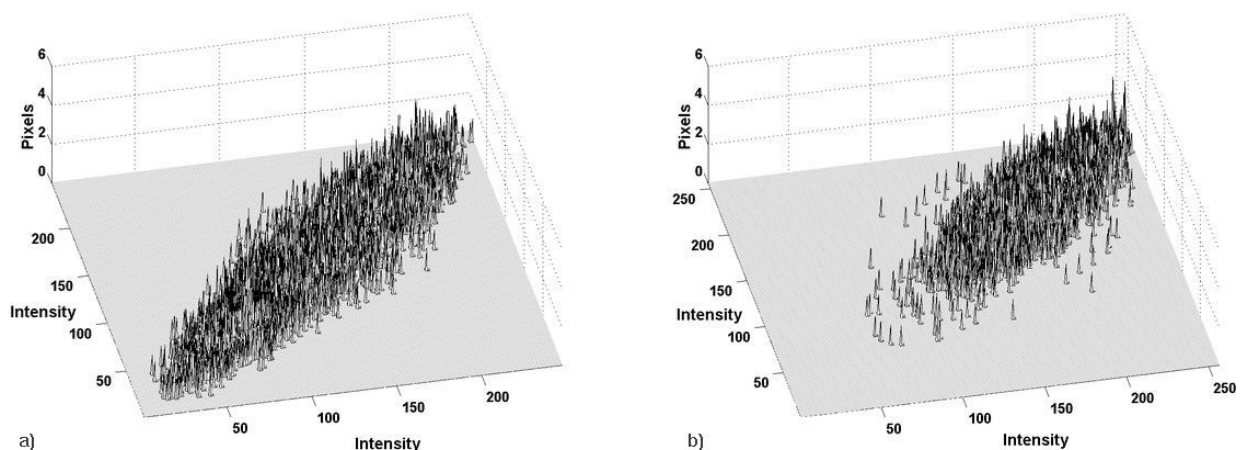


Fig. 9. The co-occurrence matrices for the tumours of the figure 8 with  $d=(0,1)$ .

## Discussion

The methods for intraocular tumour images parameters calculation and image enhancement is based on two consecutive steps: 1) inverse filtering of the image with the use of a-priori information about space varying resolution in form of point spread function; 2) calculation of multidirection statistics of the image texture with the use co-occurrence matrix.

The accuracy and result of the first step depends on the adequacy of a-priori information about PSF. In clinical environment it is not always available explicit specifications of the ultrasonic scanners used. Therefore an alternative way – blind deconvolution, based on iterative process of likelihood estimation is presented in the case of inadequate specification or simple absence of it. Of course, two methods mentioned can be integrated as well and in addition experimental verification of PSF can be made as well. This should make inverse filtering more effective.

Inverse filtering or deconvolution of image also can be made using different technologies. Wiener filter is one of the simplest and effective. Filter parameters and noise characteristics also can be automatically calculated from the image. Important feature of deconvolution using real PSF is restoration of image resolution in all directions. This allows analysis of texture and tumour anisotropy.

Preliminary analysis of co-occurrence matrixes for different tumour kinds have shown that texture statistics differs significantly. This opens the way of further research on selection of texture parameters describing the texture peculiarities and anisotropy in most informative way. Promising differences in contrast and correlation curves derived from co-occurrence matrixes is a basis for tumour differentiation.

Concrete set of texture parameters can be defined for particular tissue characterisation purposes. This set can be used for data mining algorithms having the aim to compose the decision support tree after some learning sessions. The present study is only an initial step to the more deep analysis of ultrasonic tissue differentiation.

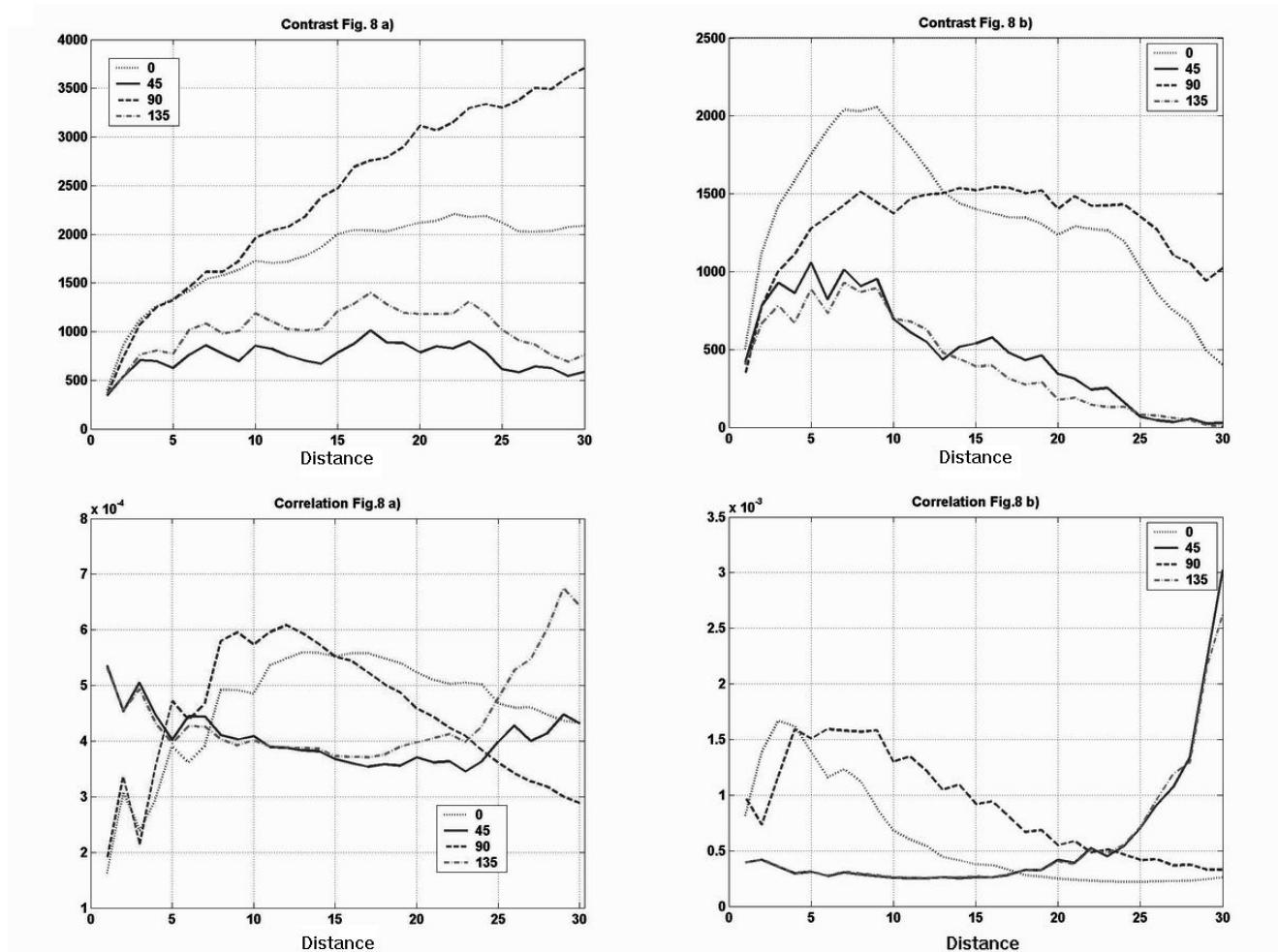


Fig. 10. Contrast and correlation distributions changing analysis distance  $d(ds, ds)$ ,  $ds=1...30$  and analysis direction. Different lines represent different directions of analysis

From practical point of view the recommended procedure for intraocular tumour ultrasound image parameterisation should be performed in this order:

- Calculation and storing of PSF by at least two proposed methods (to be accomplished by technicians, once before clinical investigations);
- Selection of the tumour region for the B-scan;
- Enhancement of the cropped tumour region by deconvolving with evaluated ultrasound systems PSF;
- Outline of the tumours boundaries or region of interest within the tumour;
- Calculation of the tumours region image texture parameters. The first step is co-occurrence matrix. The analysis of this matrix implies the choice of texture parameters to be used.

Tumour classification by ultrasonic image texture gains an interest from clinical physicians, since modern tools of image processing and decision support gives powerful tools for this problem. Wide list of possible texture parameters can be derived form co-occurrence matrix only. They can be used for modern automatic algorithms of decision support in clinical practice.

## References

1. Verbeek M., Thijssen J. M., Cuypers M. H. Echographic classification of intraocular tumours. *Acta Ophthalmol.* 1994 Vol.72. P.416-422.
2. Šebeliauskienė D., Paunksnis A. Echographic differentiation of malignant intraocular tumors. *Ultragarsas.* 2001. No.4(41). P.25-28.
3. Šebeliauskienė D., Paunksnis A., Barzdžiukas V. Color Doppler investigation of ophthalmic artery in patients with malignant intraocular tumors. *Ultragarsas.* 2001. No.1(38). P.38-41.
4. Mojsilovic A., Popovic M., Markovic S., Krstic M. Characterization of visually similar diffuse diseases from B-scan liver images using nonseparable wavelet transform. *IEEE Transactions on Medical Imaging*, Vol.17, No.4, August 1998.
5. Angelsen B. A. J. :Ultrasound imaging – waves, Signals, and signal Processing. Emantec, Trondheim.2000. Vol. 2. P.14-16.
6. Yu A., Oshiro O., Chihara K. The B-mode ultrasound image restoration to degraded images. *Ultrasound in medicine and biology.* 1994. 20, S-1. P.87.
7. Jensen J. A., Mathorne J., Gravesen T., Stage B. Deconvolution of in-vivo ultrasound B-mode images. *Ultrasonic Imaging.* 1993. Vol.15. 1993, P.122-133.
8. Abeyratne U. R., Petropulu A. P., Reid J. M., Contant E., Forsberg F. Higher order Vs. Second order statistics in ultrasound image deconvolution. *IEEE Transactions on ultrasonics, ferroelectrics and frequency control.* 1997. Vol. 44, №. 6, Nov.
9. Mentor Advent A/B ultrasound system. Instruction manual, P/N 2550-4010 Rev.B, 1997 mentor Ophthalmics, Inc.

10. **Jensen J. A.** Field: A program for simulating ultrasound systems, Paper presented at the 10th Nordic-Baltic conference on biomedical imaging published in medical & biological, Engineering & computing. 1996. Vol.34. Supplement 1. Part 1. P. 351-353.
11. **Kundur D., Hatzinakos D.** Blind image deconvolution, signal Processing magazine. May 1996. P.43-64.
12. The handbook of pattern recognition and computer vision (2nd Edition), by **C. H. Chen, L. F. Pau, P. S. P. Wang** (eds.), World Scientific Publishing Co., 1998.
13. **Singh M. and Singh S.** Evaluation of texture methods for image analysis. Proc. 7th Australian and New Zealand Intelligent information systems conference. Perth (18-21 November, 2001). P. 117-121.

D. Jegelevičius, A. Lukoševičius, A. Paunksnis, D. Šebeliauskienė

#### **Ultragarsinės echografijos vaizdų parametrizavimas akių augliams diferencijuoti**

##### Reziumė

Tiriami skaitmenizuotų echografinių arba ultragarsinių B skenavimo vaizdų kiekybiniai parametrai, svarbūs intraokulinių akies auglių tipo ir struktūros diferencinei diagnostikai. Siekiant kompensuoti neigiamą riboto erdvinio skiriamumo įtaką parametru informatyvumui, taikomas inversinis vaizdo filtravimas. Inversiniam filtrui panaudota zondojuančiojo impulso dvimatė taško sklaidos funkcija, gauta dviem nepriklausomais metodais. Parodyta, kad inversinė filtracija padidina auglio mikrostruktūrą aprašančių parametru informatyvumą. Pasiūlyti kiekybiniai vaizdo, gauto po inversinės filtracijos, parametrai. Jie naudotini diagnostinių sprendimų palaikymo programose.

Pateikta spaudai 2002 04 23

DOI: 10.5755/j01.u.42.1.8113